Vulnerability in an Excitable Medium: Analytical and Numerical Studies of Initiating Unidirectional Propagation

C. Frank Starmer,* Vladimir N. Biktashev,‡ Dimitry N. Romashko,§ Mikhael R. Stepanov,§Olga N. Makarova,§ and Valentin I. Krinsky§

* Department of Medicine (Cardiology), Duke University Medical Center Durham, North Carolina 27710 USA; § Institute of Theoretical and Experimental Biophysics, Moscow Region, Pushchino, Russia 142292; ‡ Institute of Mathematical Problems of Biology, Moscow Region, Pushchino, Russia 142292

ABSTRACT Cardiac tissue can display unusual responses to certain stimulation protocols. In the wake of a conditioning wave of excitation, spiral waves can be initiated by applying stimuli timed to occur during a period of vulnerability (VP). Although vulnerability is well known in cardiac and chemical media, the determinants of the VP and its boundaries have received little theoretical and analytical study. From numerical and analytical studies of reaction-diffusion equations, we have found that 1) vulnerability is an inherent property of Beeler-Reuter and FitzHugh-Nagumo models of excitable media; 2) the duration of the vulnerable window (VW) the one-dimensional analog of the VP, is sensitive to the medium properties and the size of the stimulus field; and 3) the amplitudes of the excitatory and recovery processes modulate the duration of the VW. The analytical results reveal macroscopic behavior (vulnerability) derived from the diffusion of excitation that is not observable at the level of isolated cells or single reaction units.

SYMBOLS AND ABBREVIATIONS

General

VP	vulnerable period (two-dimensional effects)
VW	vulnerable window (one-dimensional effects)
FHN	FitzHugh-Nagumo cable model
BR	Beeler-Reuter cable model
x	spatial coordinate
t	time
g_{Na}	maximal Na^+ conductance
g_K	maximal K^+ conductance
C	specific membrane capacity
L	length of the stimulating electrode
θ	speed of the conditioning wavefront
Θ	speed of the newly initiated test wavefront
s1	conditioning pulse
s2	test pulse to explore vulnerability
PDE	partial differential equations
ODE	ordinary differential equations

Specific for FHN-type models

u	transmembrane voltage
v	recovery variable
$f(u)$	nonlinear excitatory function
$g(u, v)$	recovery rate

Specific for analytical approach

$X_r(t)$	coordinate of the leading edge of the newly excited antegrade wavefront
x_0	left edge of the s2 electrode
x_L	right edge of the s2 electrode
v_c	critical value of the recovery variable
$U(x - \theta t)$, $V(x - \theta t)$	profile of the conditioning wave
$x_c(t)$	position of the point with the critical value $v = v_c$ at the tail of the conditioning wave
L_{eff}	effective length of the s2 electrode that includes fringe effects
d_+, d_-	corrections to the effective electrode length related to decaying propagation of newly initiated wavefronts.
$\Theta(v)$	velocity of wavefront propagating through medium with recovery state v
T_{AP}	time duration of the action potential
x_{min}	minimal possible length of propagating excitation wave
$u_n = u_n(v)$	the equilibria of the fast equation corresponding to a fixed value of the recovery variable v (rest, unstable, excited respectively) (n = 1–3).

INTRODUCTION

Cardiac vulnerability, the initiation of self-maintained spatial patterns of activation, has long been viewed as a precursor to serious and potentially life-threatening arrhythmias. However, the medium properties responsible for vulnerability remain unclear. Mines (1914) first demonstrated vulnerability of cardiac tissue by observing that critically timed stimuli can initiate self-sustained traveling waves in rings of tissue. In intact heart, such reentrant arrhythmias often degenerate into fibrillatory rhythms that can result in sudden cardiac death. Early theoretical studies by Wiener and Rosenblueth (1946), Balakhovski (1965), and Krinsky (1966) revealed conditions for forming an organizing center around which an activation wavefront could rotate, and showed that in two-dimensional media, the wavefront was a spiral. Later experimental studies

Received for publication 19 March, 1993, and in final form 10 August 1993.

Address reprint requests to C. Frank Starmer at the Department of Medicine, Cardiovascular Division, Box 3181, Duke University Medical Center, Durham, NC 27710.

0006-3495/93/11/1775/13 $2.00

in isolated superfused rabbit left atria by Allessie et al. (1973) confirmed the spiral nature of these waves. Since then, spiral waves have been observed in a number of biological systems including aggregation patterns of *Dictyostelium discoideum* (Foerster et al., 1990) and calcium waves in oocytes (Lechleiter et al., 1991).

While these studies focused on demonstrating the existence of vulnerability and characterizing the nature of spiral patterns once they were initiated, the determinants of vulnerability and the boundaries of the vulnerable period (VP) have received little study from either experimental or theoretical perspectives.

Wiener and Rosenblueth (1946) were the first to propose a theoretical mechanism of vulnerability which was biologically realistic. They suggested that in a ring of excitable cable, a continuously recirculating action potential could be initiated by a unidirectionally propagating wavefront produced by test stimulation in the wake of a previously initiated conditioning wave. Using nerve axons to approximate a one-dimensional cable, Rosenblueth et al. (1949) verified this hypothesis by initiating a unidirectionally conducted wavefront with critically timed test stimuli following the passage of a conditioning wave.

Vulnerability has typically been observed in multidimensional preparations when two conditions were met: 1) after disturbing the medium, propagation succeeds in some directions and fails in other directions and 2) there must be enough space for the spiral or recirculating waves to form (Balakhovski, 1965; Krinsky, 1966; Allessie et al., 1973; Gul'ko and Petrov, 1972; van Capelle and Durrer, 1980). When the medium exhibits these conditions, we consider it to be "vulnerable." To simplify our analyses, we have used the term, vulnerable window (VW), the one-dimensional analog to the VP, to represent the range of stimulation times associated with initiating unidirectionally propagated wavefronts, thus avoiding the complexities associated with the two-dimensional processes of spiral wave formation.

Recently, Quan and Rudy (1990) investigated vulnerability in a homogeneous one-dimensional ring of cardiac fiber using the Beeler-Reuter (1977) model of ventricular cells. Not only did they observe a range of critically timed stimuli that initiated recirculating activation, but they found that the VW was sensitive to changes in the maximum sodium conductance.

Starmer et al. (1991) adapted the Beeler-Reuter model to include use-dependent sodium channel blockade, a feature of many antiarrhythmic, anticonvulsant, and local anesthetic agents. Numerical studies of modulating effects of use-dependent Na^+ channel blockade indicated that the VW was prolonged in proportion to the unbinding time constant of the drug at the rest potential. Nesterenko et al. (1992) confirmed the sensitivity of the VW duration to several antiarrhythmic agents using strips of guinea pig right ventricle, and Starmer et al. (1992) found that cocaine and propoxyphene, both slowly unbinding use-dependent Na^+ channel blockers prolonged the VP in isolated right atrium of rabbit to a greater extent than the more rapidly unbinding lidocaine.

These numerical and experimental studies suggest a relationship between the VP and VW durations and medium properties. To further understand the mechanism of vulnerability we have combined analytical and numerical explorations of the formation of traveling wavefronts. The focus of these studies was to identify membrane properties that might reduce the VW duration and to develop an analytical expression to approximate the relationship between the VW and media properties.

Here we report the results of numerical studies with two models of excitable media: FitzHugh-Nagumo, a model with ungated channels (FitzHugh, 1961) and Beeler-Reuter, a model with gated channels (Beeler and Reuter, 1977). We found that reduction in sodium conductance amplifies the VW duration, while reduction in potassium conductance attenuates the VP duration. From our analytical studies, we demonstrated that vulnerability requires an asymmetry of excitability at the stimulation site. When this condition is met, we found that the VW could be approximated by L/θ, where L is the length of a test electrode (or stimulation field) and θ is the propagation velocity of the conditioning wave. Thus any decrease of conduction velocity such as use-dependent Na^+ channel blockade, hypoxia and membrane depolarization will prolong the VW duration.

STATEMENT OF THE PROBLEM

Previous investigators (Wiener and Rosenblueth, 1946; Gul'ko and Petrov, 1972; van Capelle and Durrer, 1980; Starmer et al., 1991) have shown that an asymmetry in the spatial distribution of excitability and recovery may lead to unidirectional block and spiral wave initiation. However, these studies focused on demonstrating the existence of spiral waves and provided little insight into the media properties that modulate the VP. Because cardiac vulnerability is known to occur during the T wave of the electrocardiogram, we hypothesized that the extent of the vulnerable period could be modulated by both the excitatory (sodium) and recovery (potassium) processes. Our numerical and analytical studies were thus designed to explore the role of these processes in modulating the boundaries of the VP.

The parameters influencing vulnerability were investigated in mathematical reaction-diffusion models of continuous excitable cable (Fig. 1). Since unidirectional conduction is a feature of vulnerability, an asymmetric distribution of excitability must exist at the stimulation electrode site. Otherwise, stimulation would reveal either bidirectional block or bidirectional conduction. To create an asymmetric spatial distribution of excitability, a conditioning wave was initiated by activating the s1 electrode at one end of the cable. Propagation of the conditioning wave from left to right was followed by a trailing wave of recovery. As this recovery wave propagated over a stimulation site in the middle of the cable (s2), excitability varied from symmetric (as the wavefront

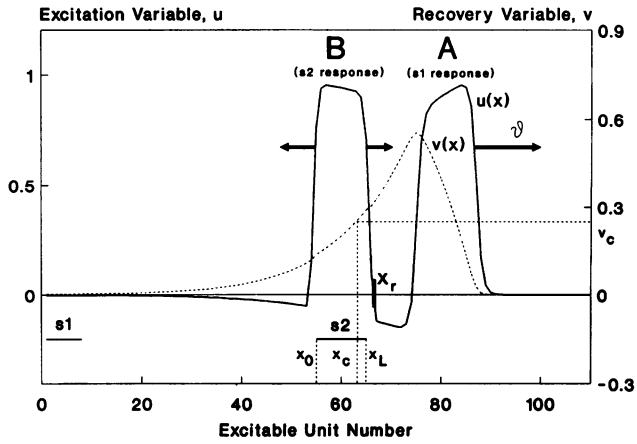

FIGURE 1 Scheme of the numerical studies of one-dimensional vulnerability. Initially, electrode s1 induces a conditioning pulse (*A*). After a delay, electrode s2 induces a test pulse (*B*). The excitation variable profile just after s2 stimulus is shown by a solid line, and the recovery variable profile at the same time is shown by a dashed line. The recovery variable profile around the s2 electrode determines the asymmetric conditions for the s2 pulse propagation. As the delay s2-s1 is increased, three classes of responses may arise: (i) pulse B decays, (ii) pulse B propagates in the retrograde direction only, (iii) pulse B divides into two pulses that propagate in opposite directions. Vulnerability is defined as the range of s2-s1 delays that exhibit case (ii) responses: unidirectional block. We have indicated the critical value of v, v_c, that separates propagating test responses from nonpropagating responses, and x_c is the position of this point. x_0 and x_L are the edges of the electrode, and X_r is the current position of the newly excited antegrade wavefront.

approaches s2) to asymmetric (as the action potential passes over s2) and returned to a symmetric distribution (as the wave moves beyond the s2 site).

We probed vulnerability with test stimuli at s2 and varied the delay between conditioning (s1) and test (s2) stimulation (s2-s1 delay). The VW was defined as the difference between the largest and smallest s2-s1 delay producing unidirectional propagation. Our problem is to explore the dependence of this quantity on the medium parameters, namely on Na^+ and K^+ conductances.

NUMERICAL METHODS AND RESULTS

We initiated our numerical studies with equations of the FitzHugh-Nagumo (FHN) type (FitzHugh, 1961). This model is a minimal model of an excitable medium and is defined in terms of a fast excitatory current and a slow recovery current and can be described by:

$$Cu_t = C\partial u/\partial t = g_{Na} f(u) - g_K v + \partial^2 u/\partial x^2$$
$$V_t = \partial v/\partial t = g(u, v) \quad (1)$$

where t is time, x is spatial coordinate, $u(x, t)$ is the transmembrane voltage (fast process), $v(x, t)$ represents the slow recovery process, C is the specific membrane capacity, $f(u)$ represents the nonlinear, N-shaped, current-voltage relationship of the excitatory process, and $g(u, v)$ reflects the dynamics of the recovery process. We introduce the parameters g_{Na} and g_K modulating the maximal excitatory and recovery currents which are similar to corresponding ion channel conductances in the Beeler-Reuter model.

The equations were integrated with the explicit Euler's method, with 110 equally spaced grid points arranged on the cable. In the numerical experiments, the model parameters were C = 0.06; $f(u) = 6.75u(u - 0.25)(1.0 - u)$; and $g(u, v) = u - 0.7v$.

The time and space steps of numerical integration were: $dt = 0.01$, $dx = 0.9$, respectively. The maximal potassium and sodium conductances, g_K and g_{Na}, were varied between 0 and 1, assuming that unit values correspond to "normal" medium properties. The numerical experiments were performed in dimensionless units. The dimensionless spatial and temporal results obtained (VW, L, etc.) were scaled by the factors of 0.15 s and 0.5 cm, respectively to obtain values comparable with experimental data from cardiac tissue. These values provided physiologically reasonable values for the AP duration and the velocity of the conditioning wave. This posterior choice of physical units was utilized for the FHN model because of its qualitative nature and since it was not derived from biophysical considerations. The stimulus current was simulated by a jump in membrane potential (i.e., $u \rightarrow u + 1.0$) at the stimulation sites.

We demonstrated the existence of three different classes of response to test stimulation (Fig. 2 *A–C*) with the FHN model. Here is shown the response to test stimulation when the s2-s1 delay was sufficiently short so that no new wavefronts were formed. In the middle is shown the response to test stimulation where s1-s2 was timed to occur within the VW and unidirectional propagation was observed. The lower panel illustrates bidirectional propagation, a response to s2-s1 stimulation that occurs after the VW. Here both the antegrade and retrograde wavefronts propagate in a stable manner.

Similar investigations were carried out using the Beeler-Reuter (BR) model (Beeler and Reuter, 1977)—an example of an ionic model that includes channel gating and providing results that are closer to that of cardiac tissue. The parameters for a single excitable unit were those used by Beeler and Reuter (1977), and the parameters for the cable model were those used by Starmer et al. (1991). Responses similar to those observed with the FHN model were observed (Fig. 2, *D–F*).

We investigated the dependence of the VW on the maximal conductance of sodium, g_{Na}. Shown in Fig. 3, *A* and *B*, is the effect of reduction of g_{Na} on the wave shape. The primary effect was to simultaneously reduce the upstroke of the action potential and reduce the conduction velocity. Similarly, we explored the effects of changes of g_K on the wave shape (Fig. 3 *C*) where the primary effect of its reduction was to prolong the duration of the action potential with a negligible effect on conduction velocity. Fig. 3 *D* shows the changes to the FHN wave shape which were qualitatively similar to those observed with the BR model.

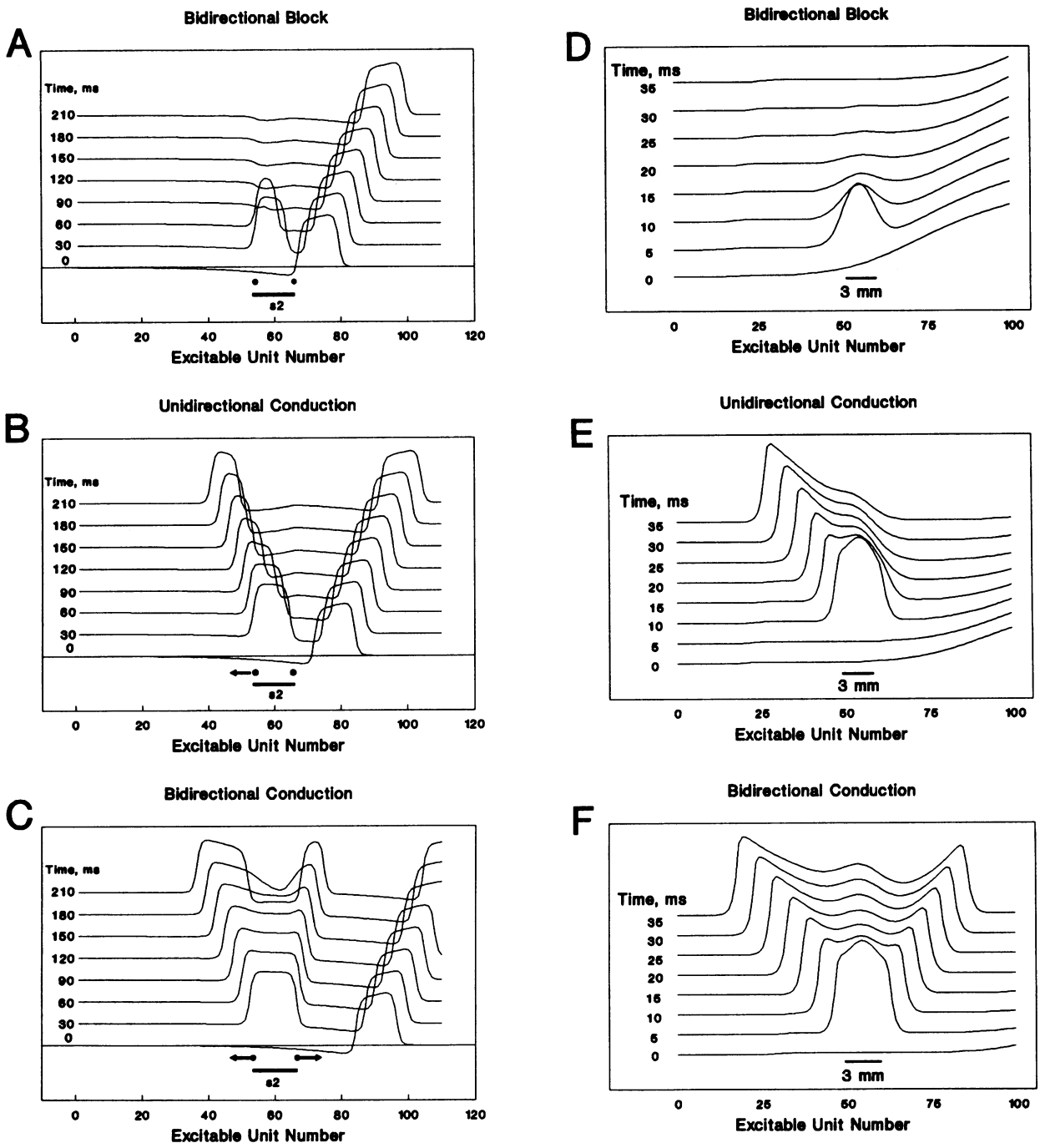

FIGURE 2 Three classes of responses to the test stimulation of the FHN (*A–C*) and BR (*D–F*) models. Shown are bidirectional block (*A* and *D*), unidirectional propagation (*B* and *E*) and bidirectional propagation (*C* and *F*). In each case, a conditioning wave is initiated by activation of the s1 electrode. Responsiveness of the cable is tested by delaying the activation of the test electrode (at time t_o) after the conditioning wave is initiated. Profiles of $u(x, t)$ are shown at increasing times just after activation of the test electrode. During propagation of the conditioning pulse, the test electrode may be activated at different times: *A* and *D* illustrate the fate of the test wave when the entire electrode is located such that $v(x, t_0) > v_c$ and no propagation is observed; *B* and *E* illustrate unidirectional propagation, a result of $v(x, t_o) = v_c$ within the boundaries of the test electrode; *C* and *F* illustrate bidirectional propagation, the result obtained when the entire test electrode spans a region where $v(x, t_o) < v_c$.

With respect to vulnerability, Fig. 4 illustrates the sensitivity of the VW duration to changes in g_{Na}. Reducing g_{Na} prolonged the duration of the VW. Modifying the medium by attenuating the excitation current revealed similar behavior of the VW for both FHN (Fig. 4 *A*) and BR (Fig. 4 *B*) excitable cables.

We found the opposite dependence for g_K, a decrease produced a reduction in the VW duration (Fig. 5). To reveal

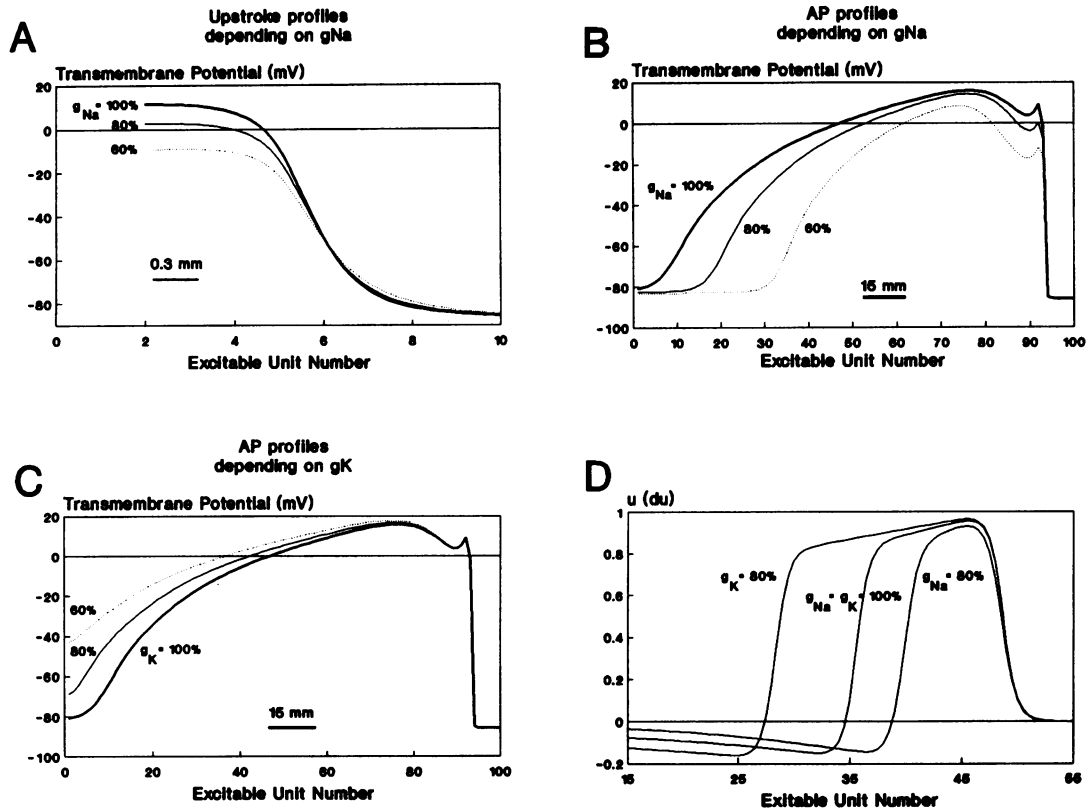

FIGURE 3 Effect of variations of g_{Na} and g_K (g_{x1} in the BR model) on wave properties. (*A*) Upstroke profiles in the BR model at different g_{Na}. (*B*) the action potential profiles at different g_{Na} (*A* is an expanded part of *B*). (*C*) Action potential profiles at different g_K. Reduction of g_{Na} diminishes the maximal value of action potential and shortens its duration. Reduction of g_K makes prolongs the action potential; its influence on the upstroke profile is negligible. *D* illustrates the effect of changes in the conductances for the FHN model. The primary effect of reducing g_K is to prolong the action potential while reducing g_{Na} prolongs the development of the wavefront and decreases its velocity.

more clearly the sensitivity of the VW to changes in g_k, we increased the VW for these studies by reducing g_{Na} by 20% for the FHN model and 40% for the BR model and then computed the VW for different values of g_k. Both FHN (Fig. 5 *A*) and BR (Fig. 5 *B*) models exhibited similar behavior.

These results support our hypothesis that vulnerability is related to the basic properties of the excitable media and that the intensities of both the excitation and recovery processes are important determinants of the VW. Since the dependencies of VW on these two parameters are qualitatively similar for rather different models, we suggest that the detailed nature of channel function is not critical for our analysis.

With respect to the mechanism of vulnerability, we hypothesize that it is primarily determined by the interaction between the field of the s2 test electrode and the recovery wave (Fig. 1). Consequently, both the conditioning pulse velocity and the length of the test electrode may modulate the VW duration. In order to understand better the mechanism of vulnerability and related dependencies, we explored the dependence of the VW on the size of the test electrode, s2 (see Fig. 6). With the exception of very small electrodes, we found the dependence to be approximately linear, both for FHN and BR models. The slope of the linear component and the x intercept were sensitive to the model parameters, g_{Na} and g_K. Namely, we found that the slope was only sensitive to g_{Na}, while the x intercept was sensitive to both g_{Na} and g_K.

A theoretical explanation of these sensitivities is proposed below. We show that the duration of the VW for large L can be approximated by the linear expression, $VW = (L + \delta L)/\theta$, where θ is the conditioning pulse velocity, L is the s2 electrode size, and δL is a relatively small correction. Thus, the dependence of the VW on g_{Na} is primarily a reflection of the dependence of θ and δL on g_{Na}, while the dependence of the VW on g_K is reflected only in the correction, δL.

ANALYTICAL RESULTS

The partial differential equations (PDE) describing a distributed excitable medium cannot be solved analytically in general (for a review, see Tyson and Keener (1988) and Mikhailov (1990)). We use here an approximate approach applicable particularly to the problem of locating the VW. The approach is most easily demonstrated for the FHN model (Eq. 1), and we restrict our attention to only this case.

We start by reviewing the qualitative nature of an action potential derived from the FHN model by consideration of the fast nullcline defined by setting $\delta u/\delta t = \delta^2/\delta t^2 = 0$ and the slow nullcline defined by setting $\delta v/\delta t = 0$ (Fig. 7*A*). The

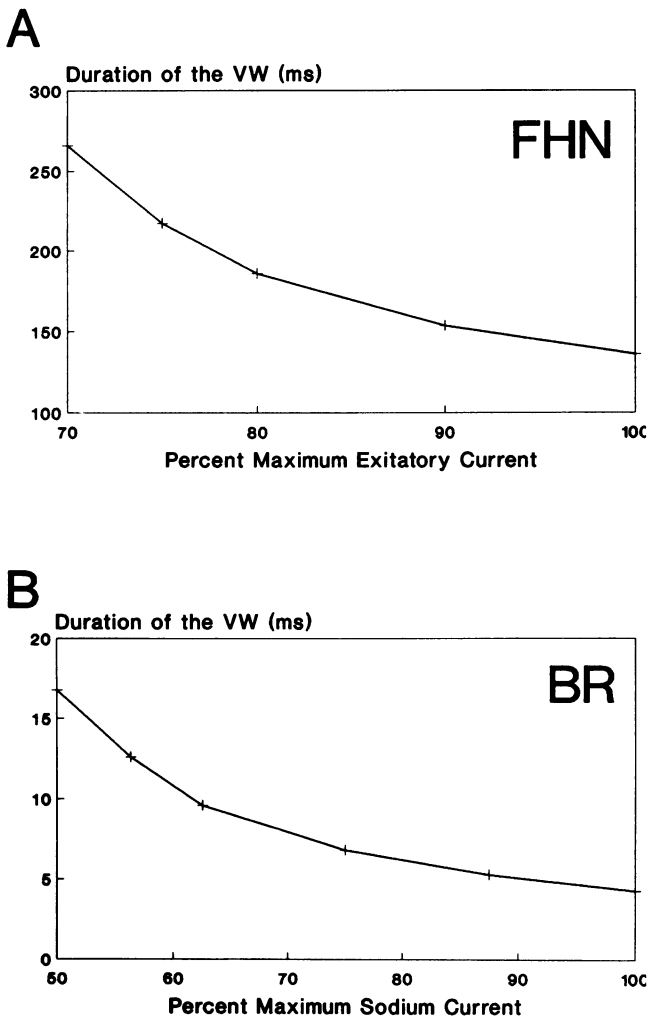

FIGURE 4 The dependence of VW on g_{Na}. Reduction of the maximum sodium (excitatory) current, g_{Na}, increases vulnerability in both the FHN (*A*) and in BR (*B*) cable models. Using the model illustrated in Fig. 1, the s2-s1 delay was varied. The VW was defined by the range of delays during which unidirectional propagation was observed.

intersection of the two nullclines defines the equilibrium condition for the membrane. Stimulation of the membrane can produce an action potential if the recovery variable, v, at this instant of time is less than a critical value, V_c (see Appendix 1). If we assume that there is a time-independent recovery process, i.e. $v(x, t) = v^* =$ constant, the propagating action potential is called a trigger wave (Fig. 7 *B*) and its velocity is dependent on the value of v^*. The amplitude of the trigger wave is determined by the intersections of the fast nullcline and the line, $v = v^*$ (Fig. 7 *A*). The minimum amplitude is fixed by the equilibrium point, u_1, while the maximum amplitude is fixed by the equilibrium at u_3.

Our approach is based on the fact that the variable v in (Eq. 1) exhibits a time course that is much slower than that of u. In FHN Eq. 1, this is provided by a small value of the membrane capacitance, C. In cardiac tissue, the excitatory process is also much faster than the repolarizing processes. The difference in time scales permits us to describe the processes of excitation and recovery by an adiabatic approximation with different formalisms (for details of formalisms see Tyson and Keener (1988) for review). Namely, we regard the dynamics of the position of the excitation wavefront, $X(t)$, as the dynamics of a trigger wave that is dependent on the local recovery state of the medium, $v(X, t)$. As the recovery state uniquely determines the velocity of trigger wave propagation, we can transform the PDE into an ordinary differential equation (ODE) and analyze the ODE for $X(t)$ at a given $v(x, t)$. The dynamics of $v(x, t)$ in (Eq. 1) have the form of an ODE for each particular x and is dependent on the dynamics of $u(x, t)$ since $u(x, t)$ forms initial conditions for $v(x, t)$ by specifying the times for "triggering" each spatial point.

The simplest estimate (zero-order approximation) for the VW duration will be obtained by considering only the initial conditions of the two potential wavefronts resulting from the s2 test pulse, i.e., their velocities in the antegrade and retrograde directions at the time instant just after stimulation (Fig. 1). A more detailed analysis of the front dynamics will

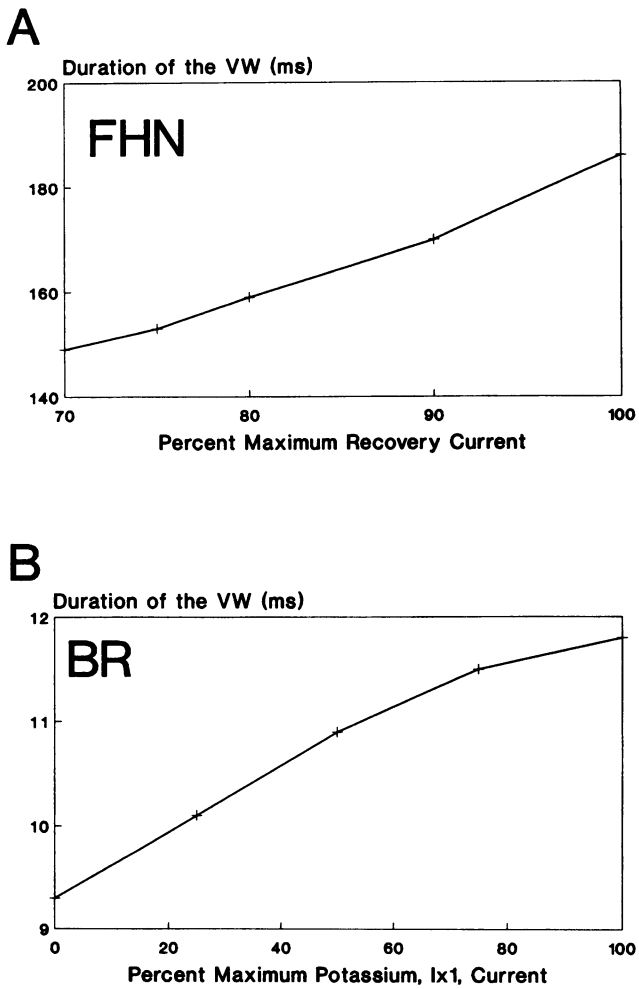

FIGURE 5 The dependence of VW on g_K. The potassium (recovery) current blockade leads to a reduction in the duration of the VW. *A* represents the sensitivity of the VW duration to reductions in g_K using the FHN model, with g_{Na} fixed at 80% of normal. *B* shows the sensitivity of the VW duration to reduction in the maximum i_{x1} current using the BR model, at g_{Na} fixed at 60% of normal.

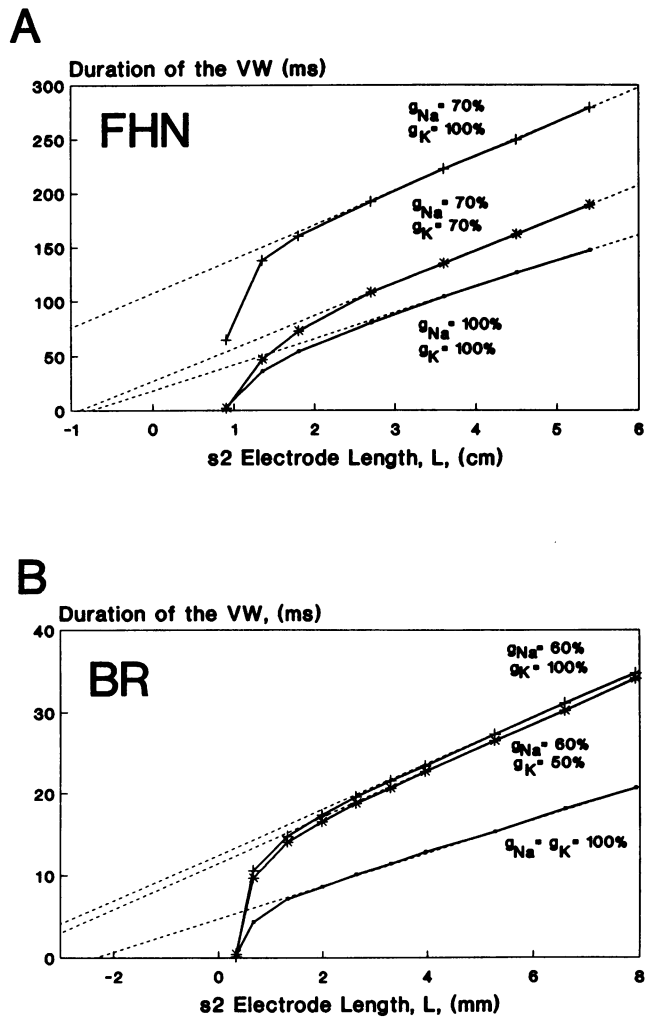

FIGURE 6 VW as a function of s2 electrode length, L. Here is shown the dependence of the VW on the length of the test electrode, s2. Note the larger the length of the electrode (L) the greater the duration of the VW. The linearity of VW (L) is exhibited only when the electrode length is significantly greater than the thickness of the wavefront; the slope of this linear dependence is reciprocal of the conditioning wave velocity. For the curves on B, the comparison of velocities measured directly and via the slope, yields (bottom to top, cm/s): 49.8 vs. 45.7, 35.1 vs. 34.5, and 35.1 vs. 34.4.

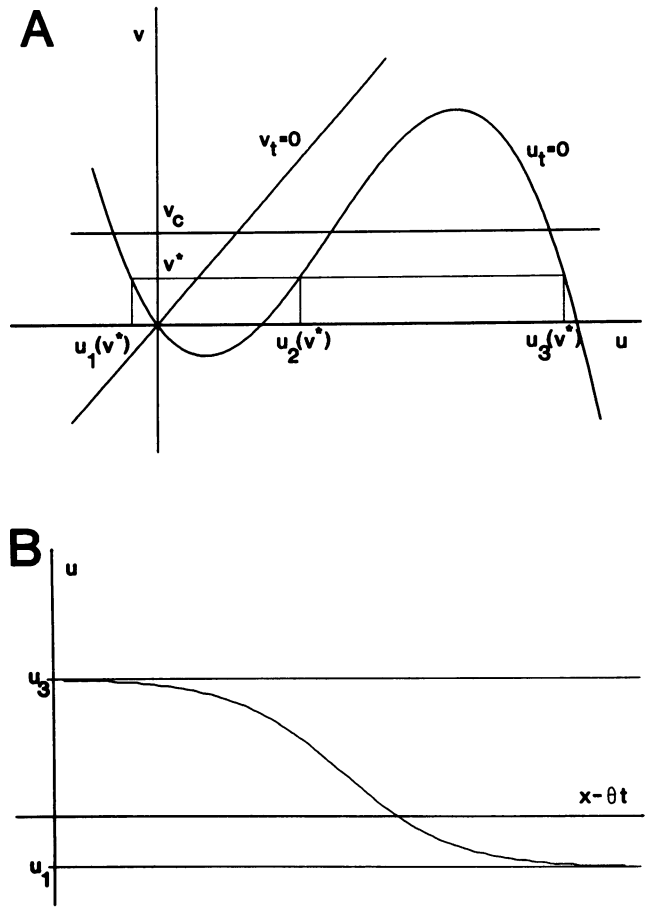

FIGURE 7 The nullclines and trigger wave in the FHN model (Eq. 1). (A) The excitatory nullcline is given by $f(u) = g_K/g_{Na}$, and recovery nullcline is given by $g(u, v) = 0$. Here, v_c, is the critical value of slow variable v that determines the fate of a propagating wavefront. The line, $v = v_c$ bisects the curve $f(u) = v$ such that the region above the line is equal in area to the region below the line. When $v > v_c$ then the boundaries of the trigger wave (represented by $u(x, t)$ of Eq. 1) exhibits negative velocity and the excited region shrinks. If $v < v_c$ then the boundaries of the trigger wave exhibits positive velocity and it propagates forward (the excited region expands). For some value, v^*, we have shown values of the equilibria in the fast equation (first of Eq. 1). Here u_2 is unstable equilibrium, u_1 and u_3 are stable, u_3 is "more stable" than u_1 (see B). (B) The trigger wave in the fast equation with some value of $v = v^*$ fixed. The wave spreads from left to right, thus triggering the medium from the "less stable" state u_1 to the "more stable" one u_3.

be made by considering the fringe effects and wavefront kinetics near the boundaries of the s2 electrode, related to decaying propagation of newly initiated waves. This yields a relatively small (first-order) correction to the zero-order approximation of the VW duration, so the resulting expression for the VW will have the form

$$\mathrm{VW} = \mathrm{VW}_0 + \mathrm{VW}_1 \quad \text{where} \quad \mathrm{VW}_1 \ll \mathrm{VW}_0 \quad (2)$$

Zero-order approximation of the VW duration

We indicate here the conditioning wave speed as θ, and the time of s2 test stimulation relative to s1 conditioning stimulation as t_0. Let the left edge of the s2 electrode be located at $x = x_0$, so the right edge is located at $x = x_L = x_0 + L$. We are to estimate the VW duration, i.e., the range of t_0 values associated with unidirectional, retrograde propagation of the newly excited test wave.

According to our assumptions that u changes much faster than v, the processes of wavefront formation and propagation may be considered as if $v(x, t)$ was constant. The front propagation velocity is then determined by the values of this constant, and we denote this dependence as $\Theta(v)$ (Fig. 8). If v is small, as it is for resting medium, the excited region expands and $\Theta(v)$ is positive. If v is large as it is in refractory medium, the excited region collapses and $\Theta(v)$ is negative. We denote the transition value of v by v_c, so that $\Theta(v_c) = 0$. This value can be determined by analysis of the first of Eq. 1 (see Appendix 1). Therefore, a wave will spread from the right edge of the electrode to the right if $v(x_L, t_0) < v_c$, and from the left edge to the left if $v(x_0, t_0) < v_c$.

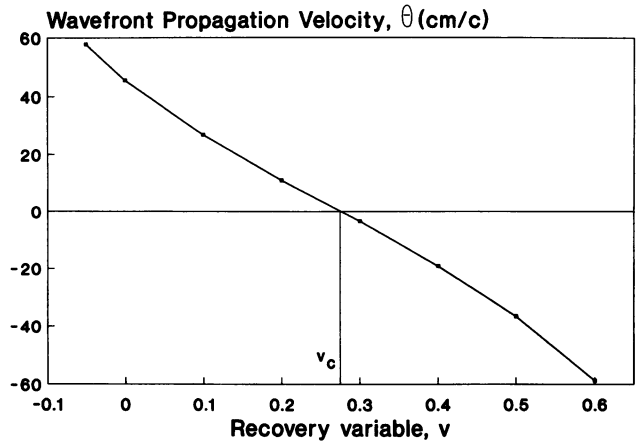

FIGURE 8 The dependence of the speed of the trigger wavefront on the value of the recovery parameter, v. The propagation velocity of the test wavefront is a function of the value of recovery variable $v(x, t)$ at the time and location of test stimulation. To show this dependence, we have computed the trigger wave velocity by numerical integrating the first of the Eq. 1 under the conditions where $v(x, t)$ = constant with stimulation at the s1 site. Shown is the velocity for values of v ranging from −0.05 to 0.6, where $g_K = g_{Na} = 1.0$. The critical value, v_c, where $\theta = 0$ is 0.27; the value of the velocity in resting medium is $\Theta(0) = 43$ cm/s. It can be seen that the dependence $\theta(v)$ is well approximated by a straight line in the region $0 < v < 2\ v_c$.

Prior to stimulation, the solution of the FitzHugh-Nagumo Eq. 1 may be formulated as

$$u(x, t) = U(x - \theta t), \qquad v(x, t) = V(x - \theta t) \tag{3}$$

a wave traveling to the right with constant velocity, θ, and with constant shape. We consider stimulation applied as the tail of the conditioning wave traverses the s2 electrode, so the profile of $v(x, t_0)$ in the vicinity of s2 is monotonic. Therefore, $v(x, t_0) > v_c$ if $x_c(t_0)$ and $v(x, t_0) < v_c$ if $x < x_c(t_0)$. Here $x_c(t)$ is the coordinate of the point on the repolarizing phase of the action potential where the slow variable equals its critical value, v_c: $v(x_c, t) = v_c$, or, according to Eq., 3

$$V[x_c(t) - \theta t] = v_c. \tag{4}$$

Thus, in the zero-order approximation, unidirectional propagation will be observed when (see Figs. 1 and 9 *A*):

$$x_0 < x_c(t_0) < x_L, \tag{5}$$

that is, the critical point x_c at the time of stimulation t_0 will be located within the boundaries of the electrode (x_0, x_L). In this case the left edge initiates an expanding front of propagating excitation while the right one initiates a collapsing wave. Choosing the fiducial time so that $x_C(0) = 0$, we get

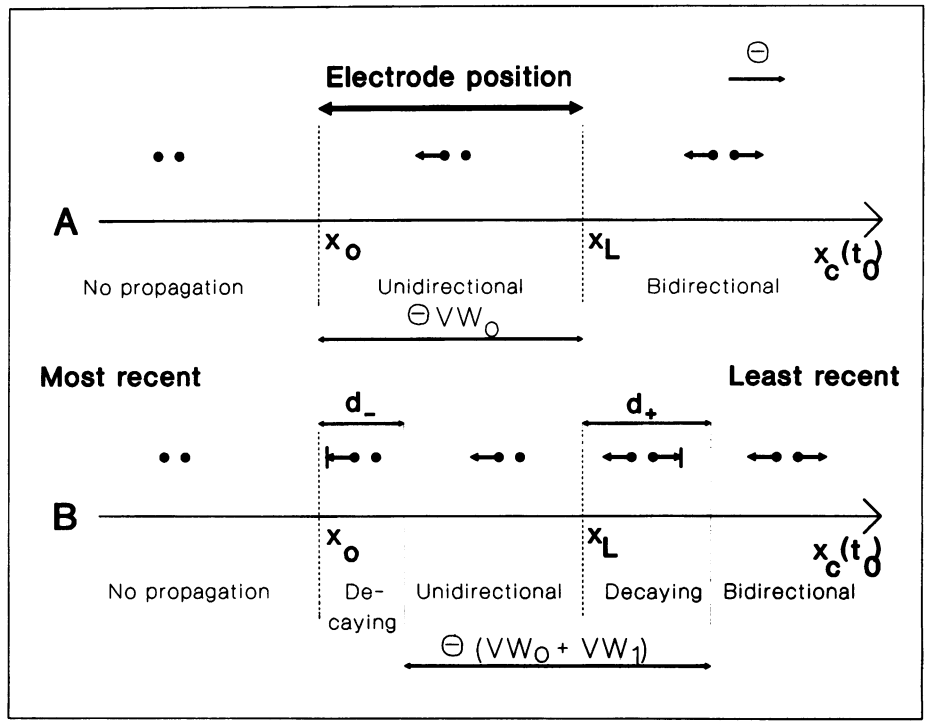

FIGURE 9 Various classes of responses depending on the time of test stimulation. The horizontal axis denotes the position of the critical point x_c at the time of stimulation relative to the position of the test electrode. This point is moving to the right with the velocity of the conditioning wave, θ. On each of two $x_c(t_0)$ axes (*A* and *B*), different possible responses to s2 stimulation are denoted. We have indicated three classes of wavefronts: ○, no wavefront formation; |←● = decaying propagation; and ←● = successful propagation. (*A*) (Upper axis) the zero-order approximation; there are three different cases (left to right): no propagation for too early stimulation, unidirectional propagation for intermediate, and bidirectional propagation for too late stimulation. The vulnerable window duration in this approximation corresponds to the electrode size divided by the velocity of the conditioning wave. (*B*) (lower axis) the first-order approximation; here we take into consideration five classes of response to s2 stimulation: the three classes indicated above and two additional cases that reflect decaying propagation between the no- and unidirectional (length d_-) and uni- and bidirectional boundaries (length d_+). In comparison to the zero-order approximation, we assume that the interval d_- in fact corresponds to no propagation, and should be excluded from the VW estimation; while the interval d_+ corresponds to unidirectional responses and should be added to the estimation. The corrected expression for the VW is $VW_0 + (d_+ - d_-)/\theta$.

that

$$x_c(t) = \theta t, \tag{6}$$

and vulnerability occurs if the stimulation time falls within the following limits:

$$0 < t_0 < L/\theta \tag{7}$$

This represents the simplest estimate for the duration of the vulnerable window,

$$VW_0 = L/\theta. \tag{8}$$

This estimate depends upon the medium properties only via the wavefront velocity (θ). Note that this velocity depends strongly upon g_{Na} and exhibits negligible dependence upon g_K, since the value of v during initiation of the conditioning wave is its equilibrium value, which is zero in Eq. 1, and g_K does not influence this velocity in the adiabatic approximation.

The numerical evidence supporting VW = L/θ is displayed in Fig. 6 for both Beeler-Reuter and FitzHugh-Nagumo models. With the exception of small L, the slopes of the curves are equal to the reciprocal wave velocity, $1/\theta$. The intersections of the tangents with the x axis are associated with changes not only in g_{Na} but also in g_K, and this dependency cannot be explained with the zero-order approximation.

First-order approximation—decaying propagation of waves dependence of VW on g_K

The zero-order approximation can be improved by accounting for more delicate phenomena that influence the effective electrode length, L_{eff}. In this section we explore the phenomenon of decaying propagation of excitation pulses, which is adequate to explain the general features of the sensitivity of the VW on g_K.

The numerical experiments demonstrate, both for FHN and BR models, that close to the boundaries of the VW, a wave initiated by the s2 stimulus may start propagating (i.e., $v < v_c$), but after a relatively short time it decays or collapses (Fig. 10). This may take place both for the antegrade and for the retrograde waves. In these cases, unidirectional propagation will take place when the condition of Eq. 7 predicts bidirectional propagation, and no propagation will occur when it predicts unidirectional propagation (see Fig. 9 *B*). Consideration of decaying propagation leads to the following correction of inequality 5:

$$x_0 + d_- < x_c(t_0) < x_L + d_+ \tag{9}$$

and of the corresponding VW estimate (Eq. 8):

$$VW = VW_0 + VW_1 = (L + d_+ - d_-)/\theta \tag{10}$$

Here d_+ (d_-) are the sizes of the regions of the following kind. When the critical point, x_c at time t_0 falls within $x_0 < x < x + d_-$, retrograde wave propagation will decay and the antegrade wave will fail to propagate while in the region, $x_L < x < x_L + d_+$, the retrograde wave will propagate and antegrade wave propagation will decay.

To evaluate the correction terms, d_+ and d_-, let us consider the antegrade wave. For convenience, we will use the term wavefront to refer to the leading edge of the traveling impulse and the term wave-back to refer to the trailing edge of the traveling impulse.

The evaluation is based on the following idealized picture (see Fig. 1). Let us consider the coordinate of the antegrade wavefront of the newly initiated wave, x_r. The velocity of this wavefront at time, t, depends on the value of the recovery variable, $v(X_r, t)$. This value is, in turn, determined by the propagation of the conditioning wave, i.e., it can be written in the form (see Eq. 3)

$$v(x, t) = V(x - \theta t) \tag{11}$$

In the adiabatic approximation, this assumption yields the following differential equation for the wavefront position, X_r, of the antegrade wave (see Fig. 1):

$$dX_r/dt = \Theta[V(X_r - \theta t)] \tag{12}$$

where $\Theta(v)$ is the velocity of the trigger wave defined by equation 1 with the slow variable, v, assumed to be constant. The typical experimental dependence of $\Theta(v)$ is shown in Fig. 8, and the critical value v_c is the solution of $\Theta(v_c) = 0$.

Given the solution of Eq. 12 with initial conditions $X_r(t_o) = x_L$ we know how far the front will be displaced in a time period equal to the action potential duration, T_{AP}. After this period, the excitation initiated by the electrode will terminate and the wave-back of the initiated pulse will form. The difference, $X_r(t_o + T_{AP}) - X_r(t_o)$ will be the initial length of the newly initiated pulse. We suggest that whether this pulse will survive or not depends upon its length. Clearly a too narrow pulse cannot survive and will decay due to inadequate excitatory current for exciting upstream elements.

So, by choosing a reasonable form for the phenomenologic functions $\Theta(v)$ and $V(x - \theta t)$ in Eq. 12, solving this differential equation for $X_r(t)$ and then solving the inequality $X_r(T_{AP}) < x_{min}$ we obtain the following estimation for d_+ (for details see Appendix 2),

$$d_+ = \begin{cases} \infty, & \text{if } \theta T_{AP} < x_{min} & \text{(i)} \\ D_+, & \text{if } \theta T_{AP} < x_{min} \text{ and } D_+ > 0, & \text{(ii)} \\ 0, & \text{if } \theta T_{AP} > x_{min} \text{ and } D_+ < 0 & \text{(iii),} \end{cases} \tag{13}$$

where D_+ is defined by the formula,

$$D_+ = x_T \log \frac{\theta T_{AP}/x_T}{\exp((\theta T_{AP} - x_{min})/x_T) - 1}, \tag{14}$$

and x_T is characteristic length of the repolarization tail, and x_{min} is characteristic width of the wavefront (see Appendix 2 for detailed description of x_T and x_{min}).

Region i corresponds to the medium that supports only decaying propagation of any pulse and, therefore, is not

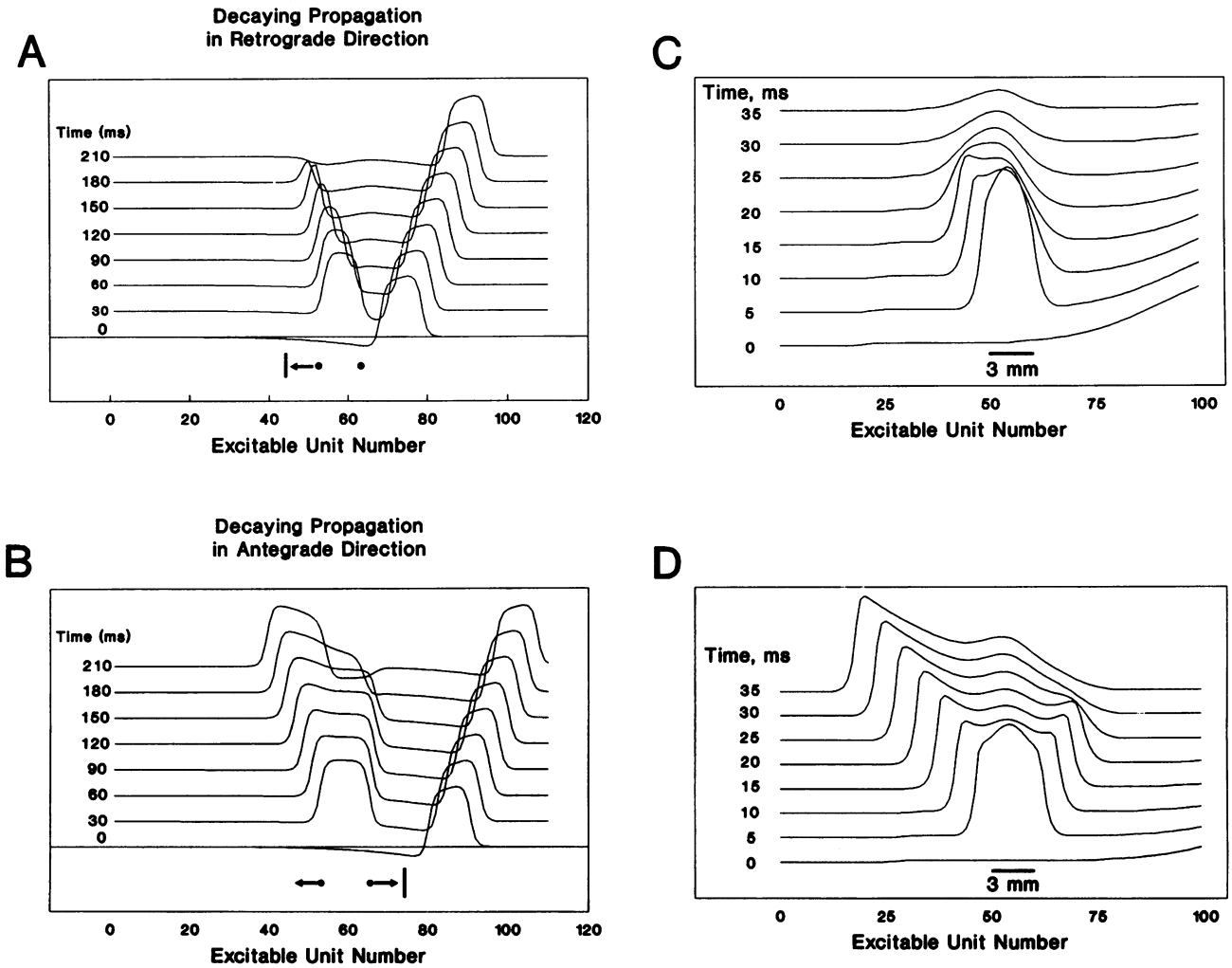

FIGURE 10 Decaying propagation of wavefronts; notations are the same as in Fig. 9. Left column, FHN model; right column, BR model. Upper row: decaying propagation of the retrograde wave initiated at a time when the zero-order approximation predicts unidirectional propagation. Lower row: decaying propagation of antegrade wave initiated where the zero-order approximation predicts a bidirectional response.

interesting for us. Region iii corresponds to the case when decaying propagation never occurs, and there is no first-order correction to the VW related to this phenomenon, i.e., the zero-order approximation remains true. The same analytical procedure may be used to estimate d_- which has appeared to be much less than d_+.

Equations 10, 13, and 14 give the first-order approximation of the VW as a function on medium properties. According to Eq. 10, VW = $(L + \delta L)/\theta$, where $dL = d_+ - d_- \approx d_+$. In contrast to the zero-order approximation which depends primarily on g_{Na}, we see that T_{AP} and x_T in Eqs. 13 and 14 strongly depend on g_K, so the first-order approximation exhibits dependencies on both parameters in question.

The dependence of $VW_1 \simeq d_+$ on g_K is not directly evident from Eqs. 13 and 14. However, it can be seen from a qualitative argument presented in Appendix 3. This approach indicated that this dependence should be generic for any model of cardiac excitability, as long as the dependence is primarily due to the effect of decaying propagation of newly initiated (test) waves.

Fig. 11 *A* illustrates the improvement in the analytical estimation of the VW as a function of electrode length, L, for the FHN model at $g_K = g_{Na} = 0.8$.

To explore the dependence of the VW on g_K, additional numerical experiments were performed by varying the parameter g_K in the FHN cable model. For this comparison, we measured, simultaneously with the VW, the phenomenological parameters T_{AP}, x_T and x_{min} appearing in expression 14. T_{AP} was the time required for the conditioning pulse to cross the midpoint of the cable, while the conditions $v > v_c$, $u > 0$ are satisfied. x_{min} was taken as the distance between points on the front of the conditioning wave where $u = 0.1$ and $u = 0.9$. x_T was the distance within the recovery tail of the conditioning wave required for an e-fold reduction in v starting from the point where

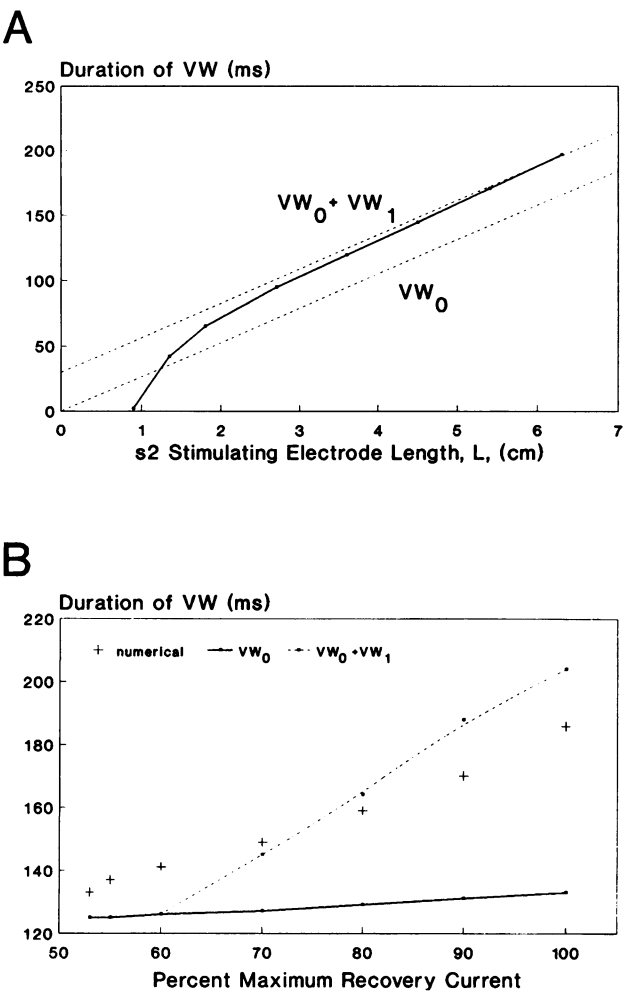

FIGURE 11 Effect of corrections to the zero order approximation. (*A*). Comparison of numerical measurements of the VW and the zero-order and first-order approximations for the FHN model, with $g_K = g_{Na} = 0.8$. In this graph, the effect of the first-order correction is to increase the apparent length of the test electrode, thus introducing a parallel shift of the zero-order approximation. *B* illustrates the sensitivity of the VW duration to the zero-order approximation and the first order approximation.

$v = v_c$. Fig. 11 *B* illustrates the sensitivity of the zero-order and first-order approximations to the VW as a function of g_K.

DISCUSSION

Recently a large clinical trial (Cardiac Arrhythmia Suppression Trial) of three antiarrhythmic agents was terminated, because two of the treatment groups experienced a rate of sudden cardiac death three times that of the control group (Cardiac Arrhythmia Suppression Trial, 1989). All three drugs (flecainide, encainide, and ethmozin) exhibit use-dependent sodium channel blockade and are characterized by slow rates of unbinding at resting membrane potentials (Campbell and Vaughan Williams, 1983; Campbell, 1983; Schubert et al., 1986). Moreover, many abused substances (e.g., cocaine (Crumb and Clarkson, 1990; Kalabas, et al., 1990), tricyclic antidepressants (Nattel, 1985), and propoxyphene (Whitcomb et al., 1989)) also block sodium channels in a use-dependent manner, exhibit slow rates of unbinding, and are associated with cardiac rhythm disturbances and sudden cardiac death. These observations indicate that there is relationship between sodium channel availability and initiation of macroscopic arrhythmias. More important, these observations suggest that sodium channel blockade may amplify cardiac vulnerability. In the present paper, we have studied the simplest explanation of the phenomenon of vulnerability and modulation of its boundaries, i.e., its one-dimensional analog, the VW, and we have described the sensitivity of the VW to channel conductances. For the FHN model, a minimal model of an excitable media, we demonstrated that the VW was prolonged by reducing the magnitude of the excitatory process and attenuated by reducing the magnitude of the recovery process. With the BR model, we found similar results: reducing g_{Na} prolongs the VW while reducing g_K attenuates the VW.

We have related these numerical results with analytical considerations of a highly relaxational FitzHugh-Nagumo model (Eq. 1) in order to find some approximations to the VW. The simplest ("zero-order") approximation we obtained is $VW = L/\theta$, where L is the test electrode size and θ is the velocity of the conditioning wave. This approximation is consistent with the earlier experimental studies where the effect of sodium channel blockade was to reduce the propagation velocity. Moreover, this result suggests that any intervention that reduces the propagation velocity (such as a small depolarization of the rest potential by ischemia or hypoxia) will also extend the vulnerable period.

Extending the analysis to include fringe effects at the boundaries of the test stimulation electrode revealed a sensitivity to the repolarizing currents. Namely, we have considered the sensitivity of decaying propagation of newly initiated fronts to medium parameters, and proposed an analytical model for considering the phenomenon of decaying propagation. Here we found this phenomenon led to consideration of an "apparent" electrode length ($L + \delta L$) and provided a satisfactory explanation of attenuation of the VW by reductions in repolarizing currents.

There are other factors that can influence the apparent electrode length, e.g., the electrotonic effect and its variability depending on the medium properties and stimulation conditions, or the details of the process of the fronts' formation. We focused here on decaying propagation, because it was most evident in our numerical experiments and led to a satisfactory qualitative description of the numerical results. Moreover, the relationships observed between the VW and medium properties, as described by the FitzHugh-Nagumo model, conformed with the results of the more realistic Beeler-Reuter model. This suggests that the qualitative explanation of the role of repolarizing currents given here generic.

Our results suggest that any reduction in conduction velocity of the conditioning wave is inherently proarrhythmic

and increases the VW. Not only sodium channel blockade but slowed conduction associated with ischemia or hypoxia can exhibit proarrhythmic effects. For this reason, we conclude that control of re-entrant arrhythmias based on potassium channel blockade should receive serious consideration based on its ability to attenuate the VW.

APPENDIX 1: ESTIMATION OF THE CRITICAL VALUE OF THE FHN RECOVERY PARAMETER, *V*, WHERE PROPAGATION VELOCITY = 0

For simplicity, we consider the FitzHugh-Nagumo model (Eq. 1) where the scale factors, g_K and g_{Na} are unity. The capacitance is assumed small so that the dynamics of the potential, u, are much faster than that of the recovery parameter, v. Under these conditions we consider $v(x, t)$ = constant and ask the question, what is the value of $v = v_c$ when propagation of a wavefront fails, i.e., $\theta = 0$?

Transforming the independent variables such that $\psi = x - \theta t$ we have

$$-\theta du/d\psi = f(u) - v_c + d^2u/d\psi^2. \tag{A1.1}$$

When a wavefront, formed by stimulation, fails to propagate, $\theta = 0$ so that

$$0 = f(u) - v_c + d^2u/d\psi^2. \tag{A1.2}$$

First we multiply each term by $du/d\psi$ and integrate from $-\infty$ to $+\infty$,

$$0 = \int_{-\infty}^{+\infty} [f(u) - v_c] \frac{du}{d\psi} d\psi + \int_{-\infty}^{+\infty} \frac{d^2u}{d\psi^2} \frac{du}{d\psi} d\psi \tag{A1.3}$$

or

$$0 = \int_{u1}^{u3} [f(u) - v_c]\, du + \int_0^0 \frac{du}{d\psi} d\left(\frac{du}{d\psi}\right), \tag{A1.4}$$

where u_1 and u_3 are the roots of the equation, $f(u) = v_c$, and are the minimum and maximum values of the trigger wave (Fig. 7, *A* and *B*). The limits of the second integral are zero since $du/d\psi$ is zero at $\psi = +\infty$ and $-\infty$ for a trigger wave. This yields

$$\int_{u1}^{u3} [f(u) - v_c]\, du = 0 \tag{A1.5}$$

This means, that when $f(u)$ is represented by any "*N*-shaped" function, the critical value occurs when the line, $v = v_c$, divides $f(u)$ into equal areas above and below this line, as shown on Fig. 7 *A*.

APPENDIX 2: ANALYTICAL ESTIMATION OF THE CORRECTION TO ELECTRODE LENGTH DUE TO DECAYING PROPAGATION

To obtain an analytical estimation for $X_r(t)$ as a solution of Eq. 12, we approximate the function, $\Theta(v)$, shown in Fig. 8, by a linear function:

$$\Theta(v) = \theta_{max}\,(1 - v/v_c) \tag{A2.1}$$

This form conserves the main properties of the function $\Theta(v)$, i.e., monotonically decreasing and a zero at $v = v_c$. The form of the repolarization tail of the conditioning wave $V(x)$ is approximated by an exponent function:

$$V(x) = v_c \exp(x/x_T) \tag{A2.2}$$

where x_T is characteristic spatial length (similar to the temporal time constant) of the repolarization tail. This latter assumption is in a good agreement with experimental data and, formally, is equivalent to linearizing the repolarization process in Eq. 1 in the vicinity of the equilibrium point. The factor v_c in Eq. A2.2 is chosen to match the condition $V(t = 0, x = 0) = v_c$.

With this assumption, Eq. 12 can be solved analytically, and the solution with the initial condition $x_r(t_o) = x_L$ is

$$X_r(t) = x_L + \theta(t - t_0) - x_T \log\left(1 + \frac{\theta(t - t_0)}{x_T} e^{(L - \theta t_0)/x_T}\right) \tag{A2.3}$$

The wave spreads to the right at $t = t_o$ if only $t_o > L/\Theta$, i.e., critical point at this moment is ahead of the right edge of the electrode. This is the first condition for the decaying propagation of the antegrade wave.

The nontrivial condition for decaying propagation to occur is derived from the requirement, mentioned above, that the antegrade wavefront should not propagate far enough to survive after creation of the antegrade wave-back:

$$x_r(t_0 + T_{AP}) - x_L < x_{min} \tag{A2.4}$$

The critical distance x_{min}, or critical wave width cannot be obtained in terms of our phenomenological theory and must be determined from the "microscopic" Eq. 1. We adopt here a rough estimation for this critical distance to be equal to the wavefront width (it is clear that any estimation of x_{min} value cannot be less than this quantity).

Thus, for decaying propagation of an antegrade wave, test stimulation time at s2, t_o, should satisfy the following conditions: (i) $L/\theta < t_0 < +\infty$, if $\theta T_{AP} < x$; (ii) $L/\psi < t_0 < (L + D_+)/\theta$, if $\theta T_{AP} < x_{min}$ and $D_+ > 0$,l where

$$D_+ = x_T \log \frac{\theta T_{AP} / x_T}{\exp((\theta T_{AP} - x_{min}) / x_T) - 1}; \tag{A2.5}$$

(iii) no decaying propagation if $\Theta T_{AP} > x_{min}$ and $D_+ < 0$.

The correction term d_+ in Eq. 10 for the effective electrode length is, therefore,

$$d_+ = \begin{cases} \infty, & \text{if } \theta T_{AP} < x_{min} \\ D_+, & \text{if } \theta T_{AP} > x_{min} \quad \text{and } D_+ > 0, \\ 0, & \text{if} \theta T_{AP} > x_{min} \quad \text{and } D_+ < 0 \end{cases} \tag{A2.6}$$

APPENDIX 3: QUALITATIVE EXPLANATION OF VW DEPENDENCE ON G_K

Consider the antegrade wave initiated by the test stimulus. Based on the arguments in the main text, we suggest that there exist some critical value of the recovery variable, v_{c1}, which is smaller than v_c and is critical in the following sense: if v at the right electrode edge is between v_c and v_{c1}, $v_{c1} < v(x_L, t_0) < v_c$, then we have decaying propagation, and if $v(x_L, t_0) < v_{c1}$, normal propagation occurs. We can relate this assumption to our small correction, δL in electrode length, thus the smaller $(v_c - v_{c1})$ the smaller δL, the greater $(v_c - v_{c1})$ the greater δL.

Let us explore the dependence of v_{c1} on g_K. We assume that the length of the newly initiated wave, x_{min}, is a critical parameter for its propagation—a too narrow pulse cannot survive and will decay. By definition, the wavefront will spread to the distance x_{min} if the v value at the time when the test wavefront is initiated equals v_{c1}, i.e., its initial velocity is $\Theta_{c1} = \Theta(v_{c1})$. If we assume, for rough estimation, that this velocity remains constant during this propagation, we get

$$x_{min} = \Theta_{c1} \times T_{AP}. \tag{A3.1}$$

where T_{AP} is the action potential duration. On the other hand, we suggest x_{min} can be estimated from the characteristic width of the wavefront and, therefore, independent of g_K. Therefore, Eq. A3.1 claims that the product Θ_{c1} by T_{AP} remains constant with g_K varying.

g_K strongly influences the AP duration, $T_{AP} = T_{AP}(g_K)$, and reducing g_K will prolong T_{AP}. We know that the velocity of a newly initiated pulse is strongly dependent on the value of v. So, if we decrease g_K, then T_{AP} in Eq. A3.1 will increase and Θ_{c1} will decrease. Since $v_{c1} = \Theta^{-1}(\Theta_{c1})$, then v_{c1} must increase and we see that the difference $(v_c - v_{c1})$ will diminish. In other words, the region of decaying propagation will diminish if g_K diminishes.

This research was supported in part by funds from the National Institutes of Health, HL32994 (NHLBI), the North Carolina Board of Science and

Technology, grant 92-IN-4 (C. F. Starmer), and from the Russian Fund for Fundamental Research, grant 32-011-1608 (V. N. Biktashev), grant 93-04-20951 (V. I. Krinsky, O. N. Makarova, M. R. Stepanov).

REFERENCES

Allessie, M. A., F. I. M. Bonke, and J. G. Schopman. 1973. Circus Movement in rabbit atrial muscle as a mechanism of tachycardia. *Circ. Res.* 33: 54–62.

Balakhovski, I. S. 1965. Several modes of excitation movement in ideal excitable tissue. *Biofizika.* 10:1063–1067.

Beeler, G. W., and H. Reuter. 1977. Reconstruction of the action potential of ventricular myocardial fibers. *J. Physiol.* 268:177–210.

Campbell, T. J. 1983. Resting and rate-dependent depression of maximum rate of depolarization (dv/dt(max)) in guinea-pig ventricular action potentials by mexiletine, disopyramide and encainide. *J. Cardiovasc. Pharmacol.* 5:291–296.

Campbell, T. J., and E. M. Vaughan Williams. 1983. Voltage- and time-dependent depression of maximum rate of depolarization of guinea-pig ventricular action potentials by two new anti-arrhythmic drugs, flecainide and lorcainide. *Cardiovasc. Res.* 17:251–258.

The Cardiac Arrythmia Suppression Trial (CAST) investigators. 1989. Preliminary report: effect of encainide and flecainide on mortality in a randomized trial of arryhthmia suppression after myocardial infarction. *N. Engl. J. Med.* 321:406–412.

Crumb, W. J., and C. W. Clarkson. 1990. Characterization of cocaine-induced block of cardiac sodium channels. *Biophys. J.* 7:589–599.

FitzHugh, R. 1961. Impulses and physiologic states in theoretical models of nerve membrane. *Biophys. J.* 1:445–466.

Foerster, P., S. C. Muller, and B. Hess. 1990. Curvature and spiral geometry in aggregation patterns of Dictyostelium discoideum. *Development.* 109:11–16.

Gul'ko, F. B., and A. A. Petrov. 1972. Mechanism of the formation closed pathways of conduction in excitable media. *Biofizika.* 17:261–270.

Kalabas, J. S., S. M. Blanchard, Y. Matsuyama, J. D. Long, G. W. Goffman, E. H. Ellinwood, P. K. Smith, and H. C. Strauss. 1990. Cocaine-mediated impairment of cardiac conduction in the dog: a potential mechanism for sudden death after cocaine. *J. Pharmacol. Exp. Ther.* 252:185–191.

Krinsky, V. I. 1966. Spread of excitation in an inhomogeneous medium (state similar to cardiac fibrillation) *Biofizika.* 11:676–683.

Lechleiter, J., S. Girard, E. Peralta, and D. Clapham. 1991. Spiral calcium wave propagation and annihilation in Xenopus laevis oocytes. *Science (Wash. DC).* 252:123–126.

Mikhailov, A. S. 1990. Foundations of Synergetics: 1 Distributed Active Systems, Springer-Verlag.

Mines, G. R. 1914. On circulating excitations in heart muscles and their possible relation to tachycardia and fibrillation. *Trans. Roy. Soc. Can.* 4:43–53.

Nattel, S. 1985. Frequency-dependent effects of amitriptyline on ventricular conduction and cardiac rhythm in dogs. *Circulation.* 72:898–906.

Nesterenko, V. V., A. A. Lastra, L. V. Rosenshtraukh, and C. F. Starmer. 1992. A proarrhythmic response to sodium channel blockade: modulation of the vulnerable period in guinea pig ventricular myocardium. *J. Cardiovasc. Pharmacol.* 19:810–820.

Quan, W., and Y. Rudy. 1990. Unidirectional block and reentry of cardiac excitation: a model study. *Circ. Res.* 66:367–382.

Rosenblueth, A., J. Alanis, and J. Mandoki. 1949. The functional refractory period of axons. *J. Cell. Comp. Physiol.* 33:405–440.

Schubert, B., S. Hering, R. Bodewei, L. V. Rosenshtraukh, and A. Wollenberg. 1986. Use and voltage-dependent depression of ethmozine (moricizine) of the rapid inward sodium current in single rate ventricular muscle cells. *J. Cardiovasc. Pharmacol.* 8:358–366.

Starmer, C. F., A. R. Lancaster, A. A. Lastra, and A. O. Grant. 1992. Cardiac instability amplified by use-dependent Na channel blockade. *Am. J. Physiol.* 262:H1305–1310.

Starmer, C. F., A. A. Lastra, V. V. Nesterenko, and A. O. Grant. 1991. A proarrhythmic response to sodium channel blockade: theoretical model and numerical experiments. *Circulation* 84:1364–77.

Tyson, J. J., and J. P. Keener. 1988. Singular perturbation theory traveling waves in excitable media (a review). *Physica D.* 32:327–361.

van Capelle, F. J. L., and D. Durrer. 1980. Computer simulation of arrhythmias in a network of coupled excitable elements. *Circ. Res.* 47:454–466.

Whitcomb, D. C., F. R. Gilliam, C. F. Starmer, and A. O. Grant. 1989. Marked QRS complex abnormalities and sodium channel blockade by propoxyphene reversed by lidocaine. *J. Clin. Invest.* 84:1629–1636.

Wiener, N., and A. Rosenblueth. 1946. The mathematical formulation of the problem of conduction of impulses in a network of connected excitable elements, specifically in cardiac muscle. *Arch. Ins. Cardiol. Mex.* 16: 205–265.